

Electron-Proton Scattering at High-Momentum Transfer*

K. BERKELMAN, M. FELDMAN, R. M. LITTAUER, G. ROUSE, AND R. R. WILSON

Laboratory of Nuclear Studies, Cornell University, Ithaca, New York

(Received 28 January 1963)

The elastic electron-proton scattering cross section has been measured at laboratory angles between 90° and 144° and for values of the four-momentum transfer squared between 25 and 45 F^{-2} (incident electron laboratory energies from 830 to 1360 MeV). Both the scattered electrons and the recoil protons were momentum analyzed and counted in coincidence, making possible background-free measurements down to cross sections of the order of $10^{-36} \text{ cm}^2/\text{sr}$. The data are consistent with the Rosenbluth formula, and the resulting form factors tie on well with previous measurements at lower momentum transfer, continuing the established trend.

INTRODUCTION

IN the past decade a considerable mass of data has been obtained from the elastic scattering of high-energy electrons by protons, chiefly by Hofstadter and collaborators^{1,2} at the Stanford linear accelerator, and more recently by groups at the Cornell synchrotron³ and the Orsay linear accelerator.⁴ The early experiments involving values of the invariant four-momentum transfer squared⁵ up to $q^2 = 16 \text{ F}^{-2}$ showed a considerable reduction in the measured cross sections relative to the cross sections predicted for a point proton, indicating a spreading of the proton charge and magnetic moment. Later experiments at higher momentum transfers revealed a difference in the electric and magnetic distributions. Comparison of the electron-proton data with data obtained by scattering electrons off neutrons bound in deuterium^{6,8} enabled one to separate the isoscalar and isovector nucleon form factors. Both showed the rapid decrease with increasing momentum transfer characteristic of a 0.8 F rms nucleon radius. This behavior was qualitatively explained in terms of the exchange of vector mesons, the ω and the ρ .⁷ Recent experimental results^{2,8} in the region of $q^2 = 30 \text{ F}^{-2}$, however, have suggested possible deviations from the Rosenbluth formula at high momentum transfers, thereby complicating the analysis in terms of form factors.

Until recently, electron-proton scattering data have

generally been obtained by observing the scattered electron only. At very high values of momentum transfer, however, it becomes difficult to distinguish the elastically scattered electrons from the more abundant pions and inelastically scattered electrons, especially if a polyethylene target is used in place of pure hydrogen. In the present experiment both the scattered electron and the recoil proton were momentum analyzed and detected in coincidence. The redundancy in kinematic requirements brought about a drastic reduction in the background and a considerable improvement in the accuracy obtainable.

APPARATUS

The experimental arrangement is shown in Fig. 1. A polyethylene target $\frac{1}{16}$ in. thick, located in a straight section between quadrants of the Cornell synchrotron and rotating in synchronism with the magnet excitation, intercepted the high-energy circulating electron beam at the peak of the acceleration cycle. Each electron passing through the target made several traversals before it suffered an energy loss or scattering angle large enough to cause it to leave a stable synchrotron orbit. The effective target area inferred from discoloration of the polyethylene was a few square millimeters. A graphite target was substituted for the polyethylene for background runs.

A totally absorbing ion chamber, or quantameter,⁹ integrated absolutely the bremsstrahlung emitted in the forward direction from the target. The total energy dissipated in the ion chamber, divided by the electron beam energy, is proportional to the effective product of incident electron flux and total traversal thickness (in radiation lengths) required for cross-section calculations. Photographs were taken of the bremsstrahlung spot immediately in front of the chamber to verify that there were no other sources of radiation in the vicinity of the target and to establish the zero point for scattering angle measurements. Because the ion chamber was designed to have greater response around the outer circumference to compensate for escape of shower particles out the side of the chamber, the outside region had to be shielded from direct view of the target to

* Supported in part by the Office of Naval Research.

¹ R. Hofstadter, F. Bumiller, and M. R. Yearian, *Rev. Mod. Phys.* **30**, 482 (1958); F. Bumiller, M. Croissiaux, and R. Hofstadter, *Phys. Rev. Letters* **5**, 261 (1960).

² F. Bumiller, M. Croissiaux, E. Dally, and R. Hofstadter, *Phys. Rev.* **124**, 1623 (1961).

³ R. R. Wilson, K. Berkelman, J. M. Cassels, and D. N. Olson, *Nature* **188**, 94 (1960); D. N. Olson, H. F. Schopper, and R. R. Wilson, *Phys. Rev. Letters* **6**, 286 (1961); R. M. Littauer, H. F. Schopper, and R. R. Wilson, *ibid.* **7**, 141 (1961).

⁴ P. Lehmann, R. Taylor, and R. Wilson, *Phys. Rev.* **126**, 1183 (1962); B. Dudelzak, G. Sauvage, and P. Lehmann (to be published).

⁵ We take q^2 to be positive for space-like momentum transfers. For momenta, $1 \text{ F}^{-1} = 197 \text{ MeV}/c$.

⁶ C. DeVries, R. Hofstadter, and R. Herman, *Phys. Rev. Letters* **8**, 381 (1962).

⁷ W. R. Frazer and J. R. Fulco, *Phys. Rev. Letters* **2**, 365 (1959); S. Bergia, A. Stanghellini, S. Fubini, and C. Villi, *ibid.* **6**, 367 (1961).

⁸ R. R. Wilson, in *Proceedings of the Aix-en-Provence International Conference on Elementary Particles* (Centre d'Etudes Nucleaires de Saclay, Seine et Oise, 1961), pp. 21-31.

⁹ R. R. Wilson, *Nucl. Instr.* **1**, 101 (1957).

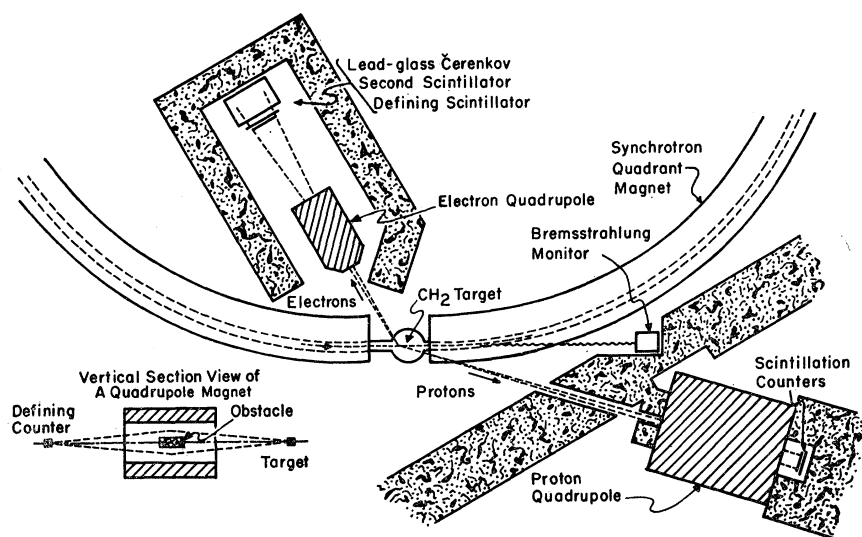


FIG. 1. Plan view of the experimental arrangement.

prevent too great a contribution from electron-positron pairs produced in the synchrotron donut wall and deflected by the fringing field. Measurements of this effect were made and a correction (7%) applied to those runs in which the extra shielding was not included. The effective area of the quantameter subtended at the target a cone of half-angle about 1.3° , implying that all but a negligible fraction of the angular distribution of emitted bremsstrahlung was intercepted. The decrease in quantameter response at high beam intensities due to ion recombination in the chamber was also measured and the monitoring for each run was corrected according to the average beam intensity for the run. This correction averaged about 4%, with an uncertainty of about one-third of the correction. The ion chamber has been intercalibrated to about 2% with other chambers,¹⁰ to 6% with a pair spectrometer,¹¹ and to 2% with a Faraday cup¹² (incident electron beam plus radiator). All results are consistent with the calibration constant 5.06×10^{18} MeV/C computed from shower theory and the specifications of the chamber.

The beam struck the target over a time spread of about 500 μ sec, centered around the peak of the 30-cps sinusoidal synchrotron magnetic field cycle. This implied an energy spread of less than 0.2%, to be added to the 0.5% spread due to slow variations of the synchrotron magnet current. The energy was monitored by integrating the magnet voltage from injection time. This has been calibrated by rotating coil measurements of the magnetic field at the beam orbit radius and checked against a pair spectrometer measurement of the bremsstrahlung spectrum¹¹ and the threshold for the reaction $\gamma + p \rightarrow K^+ + \Lambda^0$.¹³ From these measure-

ments the absolute accuracy of the beam energy calibration is estimated to be better than 1.5%. Since an error in calibration is very likely to be a slow function of energy, the effect on the experimental data is expected to be mainly a scale error common to all the data. Small errors in the beam energy can be important, since the electron scattering cross section changes by 5% for only a 1% change in energy.

Electrons emerging from the thin-walled scattering chamber passed over or under the central obstacle in a single vertically focusing large aperture quadrupole magnet of the type described by Hand and Panofsky¹⁴ (replaced by a conventional hyperbolic quadrupole of greater focusing power for the 90° measurement), and were brought to a horizontal line image of the nearly point target, the image distance depending on the momentum. The momentum defining counter, a long narrow plastic scintillator, was placed about 100 in. from the target and was followed by a second larger scintillator and a totally absorbing lead glass Čerenkov counter to select cascade showers initiated by high-energy electrons. The recoil protons were momentum analyzed in the same way using a conventional 8 in. quadrupole and two scintillation counters.

For a point target on the quadrupole axis the computed curve of detection efficiency versus magnetic field gradient for a fixed momentum particle is trapezoidal in shape; the width is determined by the vertical dimensions of the defining counter, the magnet aperture, and the obstacle. The width of the flat top of this trapezoid was chosen to be 5% or greater for both spectrometers. This relatively broad momentum resolution insured that the intrinsic elastic scattering linewidth due to finite angular aperture ($< 2\%$), target size ($< 1\%$), multiple scattering ($< 2\%$), and magnetic aberrations

¹⁰ J. W. DeWire (unpublished).

¹¹ E. Malamud (unpublished).

¹² R. Gomez, J. Pine, and A. Silverman, Nucl. Instr. (to be published).

¹³ R. Anderson (private communication).

¹⁴ L. N. Hand and W. K. H. Panofsky, Rev. Sci. Instr. **30**, 927 (1959).

(<1%) had negligible effect on the detection efficiency when the scattered momentum was centered in the resolution band, and eliminated the necessity of tracing out and integrating numerically the counting rate versus magnet current curve for each cross-section measurement. Once the magnets were calibrated, a single measurement of the coincidence counting rate at the appropriate current settings was sufficient to determine the cross section, which was then independent of momentum resolution, except for the effect on the radiation correction.

A rectangular cone about the scattered electron direction is "imaged" by the kinematics of the elastic scattering reaction into a rectangular cone about the corresponding proton direction, the vertical and horizontal opening angles each being about one-third (in the present experiment) those for the electron cone; the exact ratios vary with the incident energy and scattering angle. The magnet dimensions were such that the vertical stops and obstacle height in the proton magnet determined the vertical aperture (except in the case of the 144° measurements where it was limited on the electron side), while the length of the defining counter behind the electron magnet determined the horizontal aperture (except at 90° where it was limited by the proton counter length). The nonlimiting apertures were in all cases at least 50% oversized. The effective solid angle for scattered electrons depended on the kinematic transformation and varied from 2 to 11 msr in the experiment. Electrons were detected over a horizontal range in scattering angle of about 2.5°. Detection angles were set to better than 0.05° accuracy after a correction (as much as 2°) for the effect of the synchrotron fringe field on the recoil proton trajectories. Counter and magnet positions were set to better than 1-mm precision. Alignment was checked by varying magnet angles, incident energy, magnet currents, aperture limits, etc., and noting the effect on the coincidence rate. The focusing effect of the synchrotron fringing field on the proton detection aperture was measured by the stretched wire technique. Several cross-section measurements were repeated using different ways of defining the aperture (for example, using the electron spectrometer to define the vertical aperture) as a check on the detection solid angle. The uncertainty of the solid angle determinations is estimated at less than 3%.

An elastic scattering event was signified by a coincidence of all five counters within the resolving time of the electronics (16 nsec or less). A similar circuit with one of the input pulses delayed simultaneously monitored the accidental coincidences; these were subtracted and never amounted to more than 5%. The coincidence gated pulse-height spectrum for each of the counters was continuously displayed; none of these showed any background contamination, and the pulse-height thresholds could all be set quite comfortably low.

RESULTS

Since one of the aims of this experiment was the determination of the proton form factors as functions of the squared four-momentum transfer q^2 by measurements at a number of angles, it seemed obvious that q^2 and the scattering angle θ should be chosen as independent variables, instead of θ and the incident energy.¹⁵ Several measurements at different θ and the same q^2 can then be directly compared to determine form factors. Differential cross sections at $\theta=90^\circ, 110^\circ, 120^\circ, 130^\circ,$ and 144° were measured at $q^2=25, 30,$ and 35 F⁻². At $q^2=40$ and 45 F⁻² cross sections were measured at $120^\circ, 130^\circ,$ and 144° . These covered lab proton angles from 7.7° to 25.8° and incident electron energies from 836 to 1362 MeV. With an incident beam intensity of the order of 10¹⁰ electrons per pulse, 30 pulses/sec, the coincidence rate varied from 0.1 to 40 counts/min. Except at the highest value of q^2 , the statistical error was about 4%. The carbon background was about 2% of the hydrogen rate, and was subtracted. A correction of about 4%±2% is applied to the data to account for the nuclear absorption in the absorbers placed between the proton scintillators to reduce the singles rates.

In order to analyze the data the measured cross sections must be reduced to pure elastic scattering by subtracting the contribution of radiative scattering. Tsai¹⁶ has calculated the radiation correction for the case of electron detection including the effect of radiation by the proton (in the point-proton approximation), and Krass¹⁷ has performed the corresponding calculation for the proton detection experiment. The coincidence experiment, however introduces further complication since the two momentum resolutions impose partially overlapping restrictions on the energy of the quantum radiated.¹⁸ Table I gives the momentum resolution for

¹⁵ The incident laboratory energy, momentum transfer, and laboratory scattering angle are related by $q^2=2EE'(1-\cos\theta)=2E^2(1-\cos\theta)[1+(E/M)(1-\cos\theta)]^{-1}$, where $E, q,$ and M are in energy units.

¹⁶ Y. S. Tsai, Phys. Rev. **122**, 1898 (1961).

¹⁷ A. S. Krass, Phys. Rev. **125**, 2172 (1962). An error in Krass' calculation has been found by Abensour and Yennie (private communication). The effect of this error is less than 1% in our final cross sections.

¹⁸ In both Tsai's and Krass' expressions for the radiation correction we can separate those terms which represent the difference between lowest order pure elastic scattering and the total elastic-plus-radiative scattering (these terms being independent of spectrometer resolution, and equal in Tsai's and Krass' formulas), from those terms which account for the radiative events which are not counted either because $\Delta p_e'/p_e'$ was outside the electron spectrometer acceptance range (these terms δ_e being given by Tsai), or because $\Delta p_p'/p_p'$ was outside the proton spectrometer acceptance range (these terms δ_p being given by Krass). Because of the possibility of radiative events in which neither the electron nor the proton is detected, we would be overestimating the coincidence radiation correction if we set it equal to $\delta_e+\delta_p$. Taking it equal to the larger of δ_e and δ_p would be an underestimate except in the limit where $\delta_e\gg\delta_p$, or vice versa. Instead of making a complete calculation taking into account all the possible combinations in the kinematics of radiative scattering, we have approximated the aperture-dependent terms of the radiation correction in the ep coincidence case by expressions of the form $(\delta_e^2+\delta_p^2)^{1/2}$. In the present experiment we generally have either $\delta_e\gg\delta_p$ or vice versa, so that the error in using this approximation is expected to be rather small—less than 3% in the corrected cross sections.

TABLE I. Spectrometer momentum apertures (half-width at half-height) and calculated radiation corrections.

q^2 (F^{-2})	θ	$\Delta p_e'/p_e'$ (%)	$\Delta p_p'/p_p'$ (%)	$-\delta = \sigma_{\text{corr}}/\sigma_{\text{expt}} - 1$
25	90°	6.1	4.3	0.168
	110°	20.1	5.6	0.114
	120°	17.9	5.6	0.119
	130°	16.8	5.6	0.123
	144°	4.4	12	0.146
30	90°	5.8	4.3	0.174
	110°	18.3	5.6	0.118
	120°	16.9	5.6	0.124
	130°	15.8	5.6	0.128
	144°	4.4	13	0.142
35	90°	5.5	4.3	0.179
	110°	17.4	5.6	0.125
	120°	15.9	5.6	0.129
	130°	15.0	5.6	0.132
	144°	4.4	14	0.141
40	120°	15.2	5.6	0.134
	130°	14.2	5.6	0.137
	144°	4.4	15	0.138
45	120°	14.4	5.6	0.137
	130°	13.5	5.6	0.141
	144°	4.4	16	0.137

scattered electrons and recoil protons and the amount of the resultant radiation correction for each data point. The resolution is taken to be the half-width at half-efficiency. The correction for loss of events in which the incoming or outgoing electron makes a radiative collision with another nucleus in the target is less than 1%.

Instrumental errors in the measurements can arise from the synchrotron energy calibration, the incident flux determination, the detection solid angle calculation, the radiation correction, and the absorption correction. That part of the instrumental error which can be expected to vary randomly from one measurement to the next was estimated conservatively to be less than about 6% and was combined with the statistical error before

TABLE II. Experimental data, after radiation correction.

q^2 (F^{-2})	θ	E (MeV)	θ_p	$d\sigma/d\Omega$ (10^{-34} cm ² /sr)	$\sigma_{NS}^{-1}d\sigma/d\Omega$
25	90°	1003	25.8°	14.22±0.87	0.286±0.017
	110°	913	19.5°	6.78±0.46	0.344±0.023
	120°	887	16.5°	6.45±0.34	0.532±0.028
	130°	863	13.6°	5.32±0.32	0.723±0.045
	144°	839	9.7°	3.77±0.29	1.141±0.090
30	90°	1134	24.4°	8.23±0.52	0.226±0.015
	110°	1040	18.4°	4.50±0.34	0.319±0.024
	120°	1011	15.5°	3.80±0.20	0.441±0.023
	130°	979	12.8°	3.23±0.22	0.614±0.042
	144°	959	9.0°	2.30±0.16	0.980±0.073
35	90°	1263	23.1°	4.08±0.33	0.147±0.012
	110°	1161	17.4°	2.39±0.23	0.224±0.021
	120°	1128	14.6°	2.00±0.12	0.311±0.019
	130°	1102	12.1°	1.87±0.16	0.489±0.040
	144°	1076	8.5°	1.21±0.11	0.704±0.064
40	120°	1248	13.9°	1.37±0.10	0.278±0.020
	130°	1217	11.5°	1.21±0.09	0.410±0.030
	144°	1191	8.2°	0.73±0.08	0.555±0.062
	120°	1362	13.2°	0.71±0.08	0.108±0.020
45	130°	1331	10.9°	0.65±0.08	0.281±0.024
	144°	1305	7.7°	0.54±0.11	0.529±0.100

determining the form factors from the cross sections. The remaining systematic errors constituted a scale uncertainty common to all the measurements. This was estimated to be at most 10% in the cross sections or about 5% in the form factors, and was included only after the form factors were determined.

The corrected cross sections are given in Table II and Fig. 2. The data tie on well with the extrapolation of Stanford² and Cornell³ data at lower momentum transfers, but differ somewhat from previously published Cornell data above $q^2=25$ F^{-2} , presumably because of the background difficulties encountered in the earlier experiment.

THE ROSENBLUTH FORMULA

The laboratory differential cross section for the elastic scattering of electrons by protons has been derived from conventional quantum electrodynamics to lowest order in α by Rosenbluth¹⁹:

$$d\sigma/d\Omega = \sigma_{NS} \{ F_1^2 + \tau [2(F_1 + \kappa F_2)^2 \tan^2(\theta/2) + \kappa^2 F_2^2] \},$$

where

$$\sigma_{NS} = \left(\frac{e^2}{2E} \right)^2 \frac{\cos^2(\theta/2)}{\sin^4(\theta/2)} \frac{1}{1 + (2E/M) \sin^2(\theta/2)}$$

is the Mott differential cross section for scattering of electrons by a point charge with mass equal to the proton mass M , $\tau = q^2/4M^2$ (q^2 and M^2 in the same units), and $\kappa = 1.793$ is the proton anomalous magnetic moment in nuclear magnetons. The extended electromagnetic structure of the proton is characterized by the form factors F_1 and F_2 , which must be real functions of q^2 only (normalized to unity at $q^2=0$), and are associated, respectively, with the Dirac and Pauli interactions of the physical proton with the virtual photon exchanged. Sachs²⁰ has suggested that a more meaningful separation of the charge and magnetic moment interactions or, equivalently, longitudinal and transverse photon exchanges, can be made by re-expressing the Rosenbluth cross section in terms of helicity form factors defined by

$$G_E = F_1 - \tau \kappa F_2,$$

$$G_M = F_1 + \kappa F_2.$$

Note that G_E is normalized to unity and G_M to $1 + \kappa$ at $q^2=0$. In terms of G_E and G_M the Rosenbluth formula reads

$$d\sigma/d\Omega = \sigma_{NS} \{ (1 + \tau)^{-1} G_E^2 + \tau (1 + \tau)^{-1} G_M^2 + 2\tau [\tan^2(\theta/2)] G_M^2 \}.$$

It is clear that in either representation, the form factors at a given value of q^2 can be determined from the data at various angles θ simply by plotting $\sigma_{NS}^{-1}d\sigma/d\Omega$ vs

¹⁹ M. N. Rosenbluth, Phys. Rev. **79**, 615 (1950).

²⁰ F. J. Ernst, R. G. Sachs, and K. C. Wali, Phys. Rev. **119**, 1105 (1960); R. G. Sachs, *ibid.* **126**, 2256 (1962).

$\tan^2(\theta/2)$ and fitting to a straight line. Failure to fit a straight line with real form factors implies a breakdown in the assumptions implicit in the Rosenbluth formula.

One class of phenomena which can lead to discrepancies between the observed cross sections and the Rosenbluth formula is represented by the higher order terms in the scattering amplitude. In practice, one need worry only about the interference between these amplitudes and the Born amplitude, since their squares will be smaller by yet another power of α . Moreover, it is only the noninfrared contributions that can give rise to departures from the Rosenbluth formula; the infrared part has already been included in the radiation correction.¹⁶

Several theoretical estimates of the effect of two-photon exchange have been made. McKinley and Feshbach²¹ computed the second order Born approximation for an electron scattering from a central Coulomb potential obtaining a correction factor to the Rosenbluth cross section equal to $1 + \alpha\pi[\sin(\theta/2)]/[1 + \sin(\theta/2)]$ independent of incident energy. This is at the most only a 1% correction, and in the backward hemisphere is almost constant. On the other hand, the strong enhancement in the photon-proton elastic scattering due to the 33 pion-nucleon resonance suggests a similar enhancement of the two-photon amplitude in electron scattering. Drell and Fubini²² have shown that since the γp cross section is largely absorptive in the resonance region, the enhanced amplitude will be imaginary at the resonance and the interference with the real single photon exchange amplitude will be zero at the resonance energy and small everywhere—less than 1% according to their estimate. Because of their non-relativistic treatment of the nucleon, however, this estimate is expected to be valid only for energies below 1 BeV.

To determine the functional dependence of the two-photon exchange contribution without reference to the particular dynamics Gourdin and Martin²³ considered a partial-wave expansion for the exchanged photons. Of the $0+$, $0-$, $1+$, and $1-$ terms, the only one which can interfere with the $1-$ single-photon amplitude to give a contribution nonlinear in $\tan^2\theta/2$ is the $1+$ amplitude. Even the $1+$ interference term,

$$\begin{aligned} d\sigma/d\Omega - d\sigma_{\text{Rosen}}/d\Omega = \sigma_{NSB}(q^2)[\tan^2(\theta/2)] \\ \times [1 + (1 + \tau)^{-1} \cot^2(\theta/2)], \end{aligned}$$

is very nearly linear in $\tan^2(\theta/2)$ in the backward hemisphere and deviates appreciably from linearity only at small scattering angles. Flamm and Kummer²⁴ have postulated the existence of a spin $2+$ particle or reso-

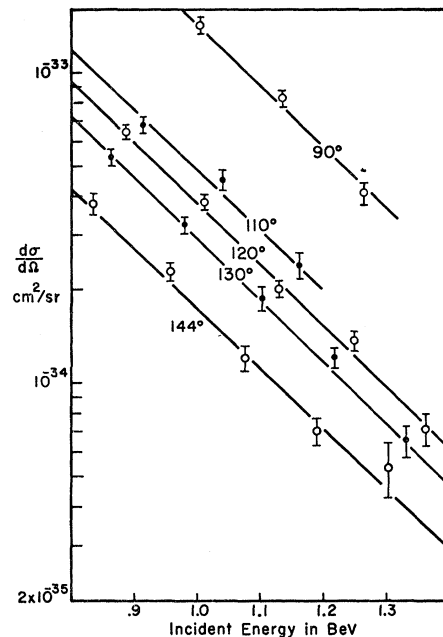


FIG. 2. Experimental differential ep scattering cross sections after radiation correction, plotted as a function of incident laboratory energy for each of the five laboratory scattering angles investigated. The 10% over-all scale uncertainty is not included in the indicated error limits.

nant state²⁵ which would intermediate between the two virtual photons and the proton. The effect on the electron scattering cross section is similar to the result obtained by Gourdin and Martin: linear in $\tan^2(\theta/2)$ except at very small angles. Although the exact mechanism or functional form involved in the contribution of the terms of higher order in α is not at present predictable, it is probably reasonable to expect that as the momentum transfer increases and the lowest order cross section becomes very small the higher terms will eventually become significant.

Deviations from the Rosenbluth formula can also come from a breakdown of the fundamental assumptions of conventional quantum electrodynamics. One can imagine, for example, a spread out electron structure, but it is impossible to separate the effects of electron and proton form factors with the electron-proton scattering data alone. A more concrete proposal by Blankenbecler, Cook, and Goldberger²⁶ suggests that the photon is not a fundamental particle of fixed angular momentum, but can be associated with a Regge pole in the same way as the strongly interacting "particles" and resonances. If we assume the same slope for the photon Regge trajectory, that is $d\alpha/ds \approx M^{-2}$, we should

²¹ W. A. McKinley and H. Feshbach, Phys. Rev. **74**, 1959 (1948).

²² S. D. Drell and S. Fubini, Phys. Rev. **113**, 741 (1959).

²³ M. Gourdin and A. Martin, Nuovo Cimento (to be published).

²⁴ D. Flamm and W. Kummer, in *Proceedings of the 1962 International Conference on High-Energy Physics at CERN*, edited by J. Prentki (CERN, Geneva, 1962), p. 216.

²⁵ This tempting in view of speculations concerning the vacuum Regge trajectory and the discovery of a meson state around 1250 MeV by W. Selove, V. Hagopian, H. Brody, A. Baker, and E. Leboy, Phys. Rev. Letters **9**, 272 (1962).

²⁶ R. Blankenbecler, L. F. Cook, and M. L. Goldberger, Phys. Rev. **128**, 2440 (1962).

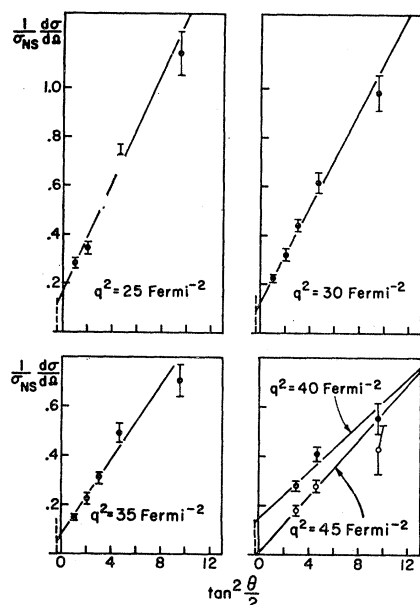


FIG. 3. Experimental values of $\sigma_{NS}^{-1} d\sigma/d\Omega$ plotted against $\tan^2(\theta/2)$ for each of the five values of momentum transfer. In each case the vertical dashed line indicates the extrapolation point $\tan^2(\theta/2) = -\frac{1}{2}(1+\tau)^{-1}$ (see text). The straight lines are obtained from least-squares fits.

expect at small scattering angles and fixed q^2 a decrease relative to the Rosenbluth cross section by a factor of $[\sin(\theta/2)]^{2q^2/M^2}$. At large angles the Regge effect is expected to be negligible; in the intermediate angular range the behavior may be more complicated, and calculations have not yet been made.

Figure 3 shows the ratio of the observed differential cross section to the Mott cross section σ_{NS} , plotted against $\tan^2(\theta/2)$ for five values of q^2 . Measurements at more forward angles would have been more useful in evaluating the theoretical speculations mentioned above, but at the high-momentum transfers investigated in this experiment smaller scattering angles require incident electron energies above the 1.4-BeV synchrotron limit. At each momentum transfer the experimental ratios are fitted rather well by a straight line. The over-all χ^2 value for eleven degrees of freedom (21 data points, minus 10 slopes and intercepts) is 19.2. The chi-squared value for each momentum transfer is given in Table III. The Rosenbluth formula also requires that the slope be non-negative (clearly this is satisfied) and that the extrapolated value at the unphysical angle $\tan^2(\theta/2) = -\frac{1}{2}(1+\tau)^{-1}$ be non-negative. This latter condition is violated by the data only at $q^2 = 45 \text{ F}^{-2}$, but even in this case the extrapolation misses being positive by a statistically insignificant amount. We, therefore, conclude that the present data show no evidence for violation of the Rosenbluth formula up to squared momentum transfers of 45 F^{-2} . This is in contradiction to the preliminary Cornell

results at high-momentum transfers (not using the e - p coincidence technique) reported at Aix-en-Provence Conference,⁸ and also contradicts the results of the Stanford group² at 145° .²⁷ Both of these earlier experiments gave inconclusive indications of an anomalously high 145° cross section at momentum transfers above 30 F^{-2} . Although the present data have laid these suspicions to rest, they unfortunately have little bearing on the theoretical predictions of departures from the Rosenbluth formula. In each case the theory predicts deviations from a linear dependence of $\sigma_{NS}^{-1} d\sigma/d\Omega$ on $\tan^2(\theta/2)$ only at far forward scattering angles. At these momentum transfers very much higher incident energies will be needed to investigate the forward scattering and thereby resolve the question of the validity of the Rosenbluth formula.²⁸

FORM FACTORS

The linear dependence shown in Fig. 3 is a necessary but *not* sufficient condition for the validity of lowest order quantum electrodynamics. Proton electric and magnetic form factors can be obtained from the straight line fits assuming the Rosenbluth formula, but it is by no means guaranteed that there is any meaning to them. Nevertheless, in the following we will assume the validity of the Rosenbluth formula.

Least-squares fits to a straight line were obtained at each of the five values of q^2 for the data shown in Fig. 3. The slope of $\sigma_{NS}^{-1} d\sigma/d\Omega$ vs $\tan^2(\theta/2)$ gives directly $2\tau G_M^2$, while the extrapolated value of $\sigma_{NS}^{-1} d\sigma/d\Omega$ at the unphysical point $\tan^2(\theta/2) = -\frac{1}{2}(1+\tau)^{-1}$ gives $G_E^2/(1+\tau)$ (recall $\tau = q^2/4M^2$). At $q^2 = 45 \text{ F}^{-2}$ the fit yields a slightly negative cross section at $\tan^2(\theta/2) = -\frac{1}{2}(1+\tau)^{-1}$ implying an imaginary value for G_E . For the purposes of discussion we set $G_E = 0$ at $q^2 = 45 \text{ F}^{-2}$ and redetermine G_M with that restriction. The best fit form factors as functions of momentum transfer are shown in Fig. 4 and Table III. The indicated error limits do not include the 5% scale uncertainty common to all the points. Also shown are the form factors simi-

TABLE III. χ^2 values and form factors derived by fitting the data to the Rosenbluth formula.

q^2 (F^{-2})	χ^2	$G_E(q^2)$	$G_M(q^2)$
25	7.7	0.396 ± 0.037	0.447 ± 0.016
30	3.1	0.359 ± 0.037	0.382 ± 0.014
35	5.1	0.258 ± 0.044	0.314 ± 0.012
40	3.1	0.436 ± 0.073	0.232 ± 0.018
45	0.2	$0 + 0.255$	0.238 ± 0.022

²⁷ These results have been superseded by the recent data of T. J. Janssens, R. Hofstadter, E. B. Hughes, and M. R. Yearian, *Bull. Am. Phys. Soc.* **7**, 620 (1962), which are in agreement with our results.

²⁸ The observation of a difference between e^+p and e^-p scattering cross sections or of a polarization of the recoil proton would also establish the presence of higher order processes.

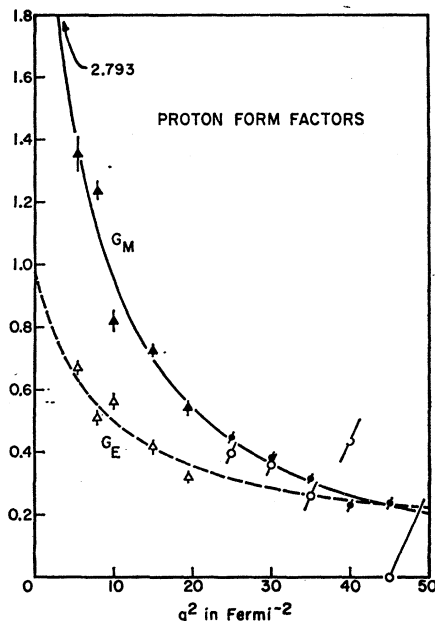


FIG. 4. The proton electric and magnetic form factors (defined in the text) as functions of the squared four-momentum transfer. The data below $q^2=20 \text{ F}^{-2}$ are taken from reference 3 (reanalyzed in terms of G_E and G_M instead of F_1 and F_2); the data above are from the present experiment. Black points represent G_M , while the open points give G_E . The 5% over-all scale uncertainty is not included in the indicated error limits. The curves are given by least-squares fits of the data here plotted to the single-resonance plus core Clementel-Villi model (see text).

larly determined from earlier Cornell data³ at lower momentum transfers. Although the determination of the form factors from the Rosenbluth formula leaves an ambiguity in sign, the normalization at $q^2=0$ and continuity enable us to conclude that G_E and G_M are positive. The measurements at backward angles have determined G_M rather well, but the uncertainties in G_E are rather large. If we had analyzed in terms of the more traditional F_1 and F_2 , the errors in both would have been large, although strongly correlated, of course. The accuracy is sufficient however, to exclude the simple hypothesis that G_E and $G_M/(1+\kappa)$ are identical functions of momentum transfer. The data are consistent with Sachs' hypothesis²⁰ that G_E and G_M approach the same constant value at very high momentum transfers, although the G_E data are not really accurate enough to make a conclusive test.

The rapid decrease in the form factors with increasing q^2 has been explained in recent years in terms of the exchange of a vector meson coupled to the virtual photon and to the nucleon.⁷ The two-pion resonance, or ρ meson, at 750 MeV²⁹ and the three-pion resonance,

or ω meson, at 780 MeV³⁰ have been observed directly in a large number of experiments, and both are known to have the 1- spin and parity and negative charge conjugation quantum number required for coupling to a photon. The scattering from the isoscalar nucleon (proton plus neutron) is expected to take place through the exchange of the $T=0$ ω meson, while the isovector nucleon (proton minus neutron) should involve the $T=1$ ρ meson. Assuming the ω and ρ resonances to be sharp, dispersion theory leads to the Clementel-Villi form factors^{31,7} for the isoscalar and isovector nucleons:

$$\begin{aligned} G_{ES} &= \frac{1}{2} - a_s + a_s / (1 + q^2/m_\omega^2), \\ G_{EV} &= \frac{1}{2} - a_v + a_v / (1 + q^2/m_\rho^2), \\ G_{MS} &= 0.440 - b_s + b_s / (1 + q^2/m_\omega^2), \\ G_{MV} &= 2.353 - b_v + b_v / (1 + q^2/m_\rho^2). \end{aligned}$$

In this approximation all higher mass exchange effects are lumped into the constant core term. The proton form factor is the sum of isoscalar and isovector, and since the ω and ρ masses are so nearly equal, we simplify by combining them in one term with a common weighting factor,

$$\begin{aligned} G_E &= 1 - a + a / (1 + q^2/m^2), \\ G_M &= 2.793 - b + b / (1 + q^2/m^2). \end{aligned}$$

If the masses of the vector meson states responsible for the electric and magnetic structures are left free to vary independently, a fair fit to the above expressions for G_E and G_M can be found³² yielding $m_E=562 \pm 35$ MeV, $m_M=474 \pm 10$ MeV, $a=0.91 \pm 0.05$ and $b=2.90 \pm 0.07$. If we impose the condition that the vector meson mass be the same for the electric and magnetic form factors, we still get an acceptable fit with $m=480$ MeV, $a=0.81$, and $b=2.91$. If we take this Clementel-Villi fit at face value, it implies that the hard-core term is a very small part of both form factors, very nearly zero within the experimental error in the magnetic case and 0.09 for the electric. If we impose the Sachs condition²⁰ that the core terms be equal and non-negative, we obtain an acceptable fit with a zero core. (The best fit is actually very slightly negative.) This would mean either that the bare proton core is practically neutral or that there is a cancellation between the core and the contribution of high mass virtual particle states. However, it is clear, upon looking at the data plotted in Fig. 4 and ignoring the Clementel-Villi formula, that each of the form factors could contain a constant core contribution as large as 0.3.

The best-fit value for the exchange vector meson mass is significantly lower than either the ω or ρ mass;

²⁹ J. A. Anderson, V. X. Bang, P. G. Burke, D. D. Carmony, and N. Schmitz, Phys. Rev. Letters 6, 365 (1961). The presently available data on the ρ meson have been summarized by G. Puppi, in *Proceedings of the 1962 International Conference on High-Energy Physics at CERN*, edited by J. Prentki (CERN, Geneva, 1962), p. 713.

³⁰ B. C. Maglič, L. W. Alvarez, A. H. Rosenfeld, and M. L. Stevenson, Phys. Rev. Letters 7, 178 (1961). More recent ω data have been summarized by G. Puppi (see reference 29).

³¹ E. Clementel and C. Villi, Nuovo Cimento 4, 1207 (1956).

³² The inclusion of electron proton scattering data from the Stanford and Orsay groups (references 2 and 4) improves the precision of the Clementel-Villi parameters, but does not significantly alter their values.

a fit to the Clementel-Villi formula with a mass around 750 MeV is completely excluded by the data. This is actually a confirmation of what we have already known from earlier Stanford^{1,2,6} and Cornell³ data. There are several ways of reconciling this with the assumed role of the ω and ρ in electron scattering. One can obtain satisfactory fits³³ by adding another resonance term to the Clementel-Villi formula, corresponding to another vector meson state of lower mass. This is dubious in the absence of evidence for the existence of such states. Nonresonant low-energy pion states give too small a contribution to be of any help. Instead, one can add a higher mass term (one or several nucleon masses, say), which by partially canceling the ω or ρ term can simulate the effect of a lower mass contribution. With a free choice of mass and amplitude one can fit almost any form factor behavior. Levinger³⁴ and Hand *et al.*³⁵ have in fact succeeded in fitting the proton form factor data (including preliminary results from this experiment) with a 750-MeV meson exchange term and a higher mass term (one or two nucleon masses), without any hardcore term.

It has also been suggested³⁶ that the functional form

³³ L. N. Hand, D. G. Miller, and R. Wilson, *Phys. Rev. Letters* **8**, 110 (1962).

³⁴ J. S. Levinger, *Nuovo Cimento* **26**, 813 (1962).

³⁵ L. N. Hand, D. G. Miller and R. Wilson (to be published).

³⁶ M. McMillan and E. Predazzi, *Nuovo Cimento* **25**, 838 (1962); G. Domokos and J. Wolf, *Phys. Letters* **1**, 349 (1962).

of the vector meson term in the Clementel-Villi formula may itself be at fault. More general expressions are derived for the form factors, in effect introducing higher powers of q^2 in the denominator of the vector meson term. In the absence of detailed information on the dynamics of the ω and ρ this simply leaves us with a few more constants to be determined from the data, thus permitting a satisfactory fit with just the ω and ρ mesons. The actual situation is probably a combination of these alternatives, that is, higher mass exchange terms and a more complex functional form; provided, of course, that it still makes sense to use the Rosenbluth formula. At present the experimental data are not sufficient to resolve all the possibilities.

Ernst, Sachs, and Wali²⁰ have shown that G_E and G_M can be expressed as Fourier transforms of the proton charge and magnetic moment spatial distributions in the Breit reference frame (the frame in which the energy transferred to the nucleon is zero). As one might expect, the Clementel-Villi vector meson term in the form factor is the transform of a Yukawa distribution. Thus our fit to G_E and G_M implies Yukawa charge and magnetic moment distributions with very small delta-function cores. Using these distributions the root-mean-square radii of the proton total charge and magnetic moment distributions come out to be $r_E = 0.82 \pm 0.04$ F and $r_M = 1.03 \pm 0.06$ F.